Chemistry–A European Journal
Research Article
doi.org/10.1002/chem.202202386
Chemistry Europe
European Chemical Societies Publishing
www.chemeurj.org

Accumulation of Four Electrons on a Terphenyl (Bis)disulfide

Lucius Schmid,[a] Igor Fokin,[b] Mathis Brändlin,[a] Dorothee Wagner,[a] Inke Siewert,*[b] and Oliver S. Wenger*[a]

Abstract: The activation of N_2, CO_2 or H_2O to energy-rich products relies on multi-electron transfer reactions, and consequently it seems desirable to understand the basics of light-driven accumulation of multiple redox equivalents. Most of the previously reported molecular acceptors merely allow the storage of up to two electrons. We report on a terphenyl compound including two disulfide bridges, which undergoes four-electron reduction in two separate electrochemical steps, aided by a combination of potential compression and inversion. Under visible-light irradiation using the organic super-electron donor tetrakis(dimethylamino)ethylene, a cascade of light-induced reaction steps is observed, leading to the cleavage of both disulfide bonds. Whereas one of them undergoes extrusion of sulfur to result in a thiophene, the other disulfide is converted to a dithiolate. These insights seem relevant to enhance the current fundamental understanding of photochemical energy storage.

Introduction

The photoinduced transfer of single electrons in donor–photosensitizer–acceptor compounds has been intensely investigated in the past decades and is now increasingly well understood.[1–10] However, for the production of solar fuels from small molecules such as H_2O or CO_2, the temporary accumulation and storage of more than one redox equivalent seems indispensable, yet proves very challenging until now.[11–16] To gain insight into the basic principles of photoinduced accumulation of redox equivalents, covalent[17–35] as well as non-covalent[36–38] molecular compounds were investigated from a fundamental mechanistic perspective. In most of the previously studied molecular multi-electron acceptors, the second reduction step is thermodynamically more challenging compared to the first one, due to electrostatic repulsion between the accumulating electrons. However, in some systems, the second reduction step is easier to accomplish than the first, a phenomenon that is called potential inversion,[39–50] and which is usually caused by significant structural changes upon two-electron reduction. Such behavior can be desirable to accumulate multiple charge equivalents, because it gives an energetic preference towards the two-electron rather than the one-electron reduced product.

A particularly interesting class of compounds showing potential inversion or two energetically similar reduction processes (i.e., potential compression) is based on the structural motif of dibenzo[1,2]dithiin and its bipyridine analogues (Figure 1).[22,51–59] This electron-acceptor has been used for light-induced charge accumulation in a molecular heptad comprised of two Ru^{II}-based photosensitizers along with four triarylamine

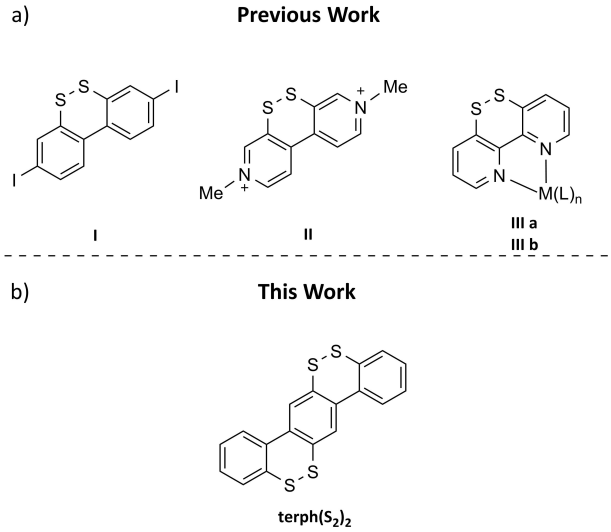

Figure 1. A selection of previously reported disulfide-based acceptors featuring potential inversion (a)[51–53,56,57] and the four-electron acceptor terph$(S_2)_2$ (b). IIIa: M = Ru^{II}, L = bpy (n = 2). IIIb: M = Re^{I}, L = CO (n = 3), Cl (n = 1).

[a] Dr. L. Schmid, M. Brändlin, D. Wagner, Prof. Dr. O. S. Wenger
Department of Chemistry
University of Basel
St. Johanns-Ring 19, 4056 Basel (Switzerland)
E-mail: oliver.wenger@unibas.ch

[b] Dr. I. Fokin, Prof. Dr. I. Siewert
University of Göttingen
Institute of Inorganic Chemistry
Tammannstrasse 4, 37077 Göttingen (Germany)
E-mail: inke.siewert@chemie.uni-goettingen.de

Supporting information for this article is available on the WWW under https://doi.org/10.1002/chem.202202386

electron donors and led to the temporary storage of two electrons on the central dibenzo[1,2]dithiin unit.[22] In separate studies, a 2,2′-bipyridine-based ligand bearing a disulfide in the backbone was coordinated to two different metals (Ru^{II} and Re^{I}, compounds III a and III b in Figure 1a), and the redox chemistry as well as the reactivity of these complexes was investigated.[52,53,57] However, the previously reported systems were based on acceptors bearing one single disulfide bond, thereby enabling the storage of a maximum of two electrons in the form of a dithiolate. One exception is compound II (Figure 1), which can undergo a fourfold reduction, however, two of the electrons are stored on the viologen scaffold, resulting in the loss of the desired potential inversion for these two reduction steps.[51] Moreover, compound II has been investigated so far only by electrochemical means, whereas the possibility of light-driven charge accumulation has remained unexplored. Due to their high density of acceptor states, nanoparticle-based and polyoxometalate systems are often competent in the accumulation of many electrons,[60–65] but in organic compounds the accumulation of more than two electrons has remained comparatively little explored.[20,28,66–69]

Herein, we present electro- and photochemical investigations of a *p*-terphenyl-based (bis)disulfide compound that represents an extension of the known molecular acceptor units from one to two disulfides (terph$(S_2)_2$, Figure 1b), in order to accumulate up to four electrons.[70] We describe the synthesis of terph$(S_2)_2$, which is then structurally characterized and thoroughly investigated in terms of its redox chemistry. Controlled potential coulometry paired with digital simulations of the cyclic voltammograms reveal two consecutive two-electron reduction processes, occurring with potential inversion and potential compression. Based on these insights, we explore the photochemical reduction of terph$(S_2)_2$ using the strong excited-state reductant tetrakis(dimethylamino)ethylene (TDAE), and we demonstrate that terph$(S_2)_2$ is indeed able to undergo photo-induced multi-electron reduction via a cascade of different reaction steps.

Results and Discussion

Synthesis and characterization

The bis(disulfide) terph$(S_2)_2$ (Scheme 1) was previously prepared following a different synthetic procedure than we employed in our work presented here.[70] The previous report did not include electrochemical studies geared at elucidating potential inversion and multi-electron storage on the terph$(S_2)_2$ compound, and no photochemical investigations were made.

Our synthetic strategy to obtain terph$(S_2)_2$ started from 1,4-dibromo-2,5-dimethoxybenzene (**1**) and boronic acid pinacol ester **2** (Scheme 1). Whereas **2** is commercially available, **1** was obtained by the bromination of 1,4-dimethoxybenzene according to a known procedure.[71] Suzuki coupling of **1** and **2** using $Pd(PPh_3)_4$ as the catalyst afforded the methoxy-protected terphenyl **3**, which was deprotected to the tetraol **4** using BBr_3. Reaction of **4** with dimethylcarbamoyl chloride ($(CH_3)_2NC(S)Cl$) in the presence of 4-(dimethylamino)pyridine (DMAP) and triethylamine ($N(Et)_3$) as a base resulted in the formation of **5** in moderate yields. Fourfold Newman–Kwart rearrangement of **5** to **6** initially proved to be difficult, because several rearrangement products were observed at the beginning of our studies. Furthermore, a thiophene species was formed as a by-product, in line with recent reports.[52] Optimization of the reaction conditions, i.e., conducting the reaction in a closed microwave vial with tetradecane as solvent led to an improved yield of 79%. Finally, **6** was deprotected with $LiAlH_4$ generating the free tetrathiol, which was then converted to bis(disulfide) terph$(S_2)_2$ using I_2 as an oxidizing agent.

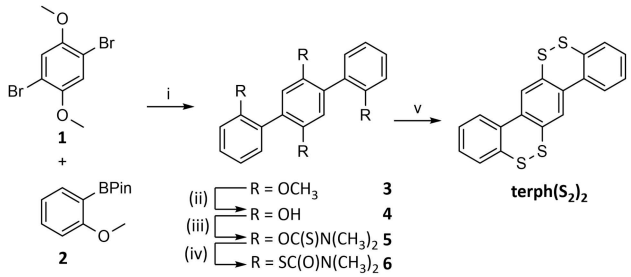

Reagents and conditions: i) $Pd(PPh_3)_4$, Na_2CO_3, toluene/EtOH, 90 °C, 16 h, 88 %; ii) BBr_3, CH_2Cl_2, −78 °C→rt, 4 h, 96 %; iii) DMAP, $(CH_3)_2NC(S)Cl$, $N(Et)_3$, 1,4-dioxane, 100 °C, 46 h, 24 %; iv) *n*-tetradecane, 260 °C, 5 h, 79 %; v) 1) $LiAlH_4$, THF, 0 °C→80 °C, 6 h; 2) I_2, THF, rt, 40 min., 57 %.

Scheme 1. Synthesis of the terphenyl (bis)disulfide key compound terph$(S_2)_2$.

Terph$(S_2)_2$ was characterized by ^1H and ^{13}C NMR spectroscopy, as well as by high-resolution mass spectrometry (HRMS) and elemental analysis (see SI, page S9). The analytical data are in good agreement with the previously reported characterization of terph$(S_2)_2$.[70] The earlier employed procedure was based on methyl-protected thiols that can be used for Pd-catalyzed C–C cross coupling reactions, which can be challenging with the typical Newman-Kwart compounds, because some of them seem to interfere with the Pd-based catalytic cycle.[72]

Electrochemistry

All electrochemical measurements were performed in N_2-saturated THF with ($^nBu_4N$)(PF_6) as supporting electrolyte and were referenced internally vs. $Fc^{+/0}$.

Cyclic voltammetry (CV) measurements on terph$(S_2)_2$ reveal two steep reduction processes, with peak potentials of −1.87 V (E_{pc1}) and −2.59 V (E_{pc2}) at a scan rate of 1 V/s (Figure 2). Both processes exhibit similar currents, indicating that the same number of electrons is transferred in both waves. The peak currents of both reduction features I_{pc1} and I_{pc2} (insets in Figure 2) increase linearly as a function of the square root of the scan rate ($v^{1/2}$), as typically observed for diffusion-controlled processes.[73] Apart from the reduction waves, a broad reoxidation feature with a peak potential $E_{pa} = -0.84$ V is observed after an initial reductive sweep (red trace in Figure 2a). Importantly, the peak current of this wave increases when the potential is

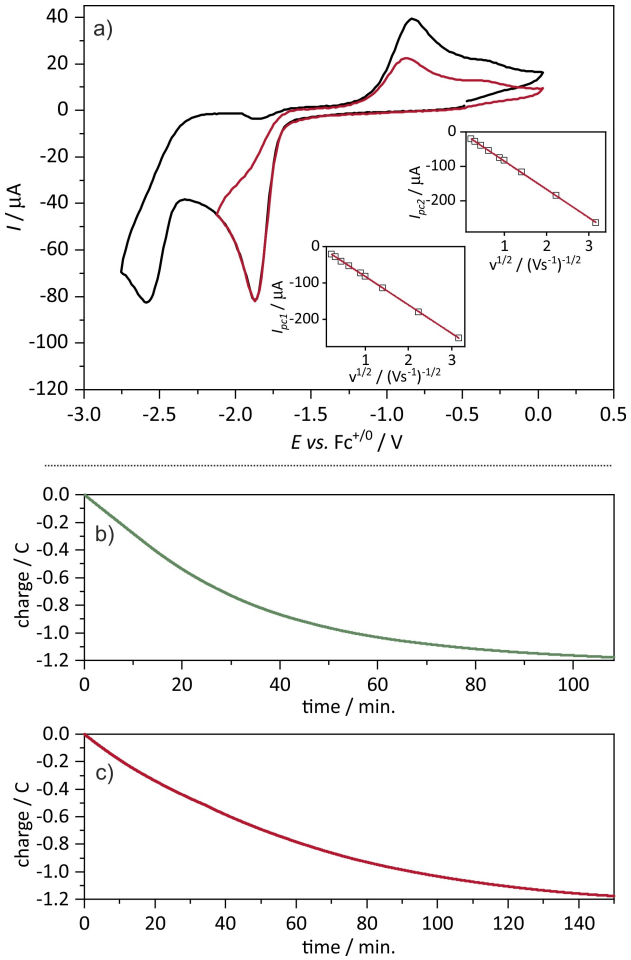

Figure 2. Top, a) Cyclic voltammograms of 1.0 mM terph$(S_2)_2$ recorded with a scan rate of 1 V/s. Insets: Plot of the reductive currents (I_{pc}) of the first (lower left) and second (upper right) reduction waves vs. the square root of the scan rate ($v^{1/2}$). Bottom: Charge vs. time curves of the coulometry experiment with terph$(S_2)_2$ at a potential between the two reduction waves (b) and at a potential more negative than the second reduction wave (c). The experiments were performed in dry, N_2-saturated THF at room temperature with 0.2 M (nBu$_4$N)(PF_6) as supporting electrolyte. For details concerning the coulometry experiments, see the main text and page S19 of the SI.

scanned beyond the second reduction process (black trace in Figure 2a), and we therefore conclude that this feature includes the reoxidations of both reduction waves. The potential separations between the individual reduction waves and the reoxidation feature are large ($\Delta E = 1.03$ V for the first and $\Delta E =$ 1.75 V for the second reduction process). This is either indicative of an irreversible redox process, for example, due to large structural changes, or an EC mechanism (E = electrochemical step, C = chemical step), in which an initial electron-transfer process is followed by a fast chemical reaction.[73] Furthermore, we observe a small oxidative feature near the second reduction feature, which gets more significant with decreasing scan rates and thus likely arises from a follow up-reaction (see below).

Previous reports on related compounds have shown that the two single-electron reduction events necessary to convert a given disulfide to its dithiolate form can occur as a single two-electron wave in cyclic voltammetry,[51–57] and, therefore, we conducted coulometry experiments to determine the number of electrons for both reduction waves observable in our bis(disulfide). At an applied potential between the two reduction waves, the current decreased to 5% after passing two charge equivalents (see SI, page S19 and Figure 2b). Subsequent coulometry at the potential required for the second reduction wave led to the injection of two additional charge equivalents (Figure 2c), thereby confirming our hypothesis that terph$(S_2)_2$ is able to store up to four electrons.

To extract the thermodynamic and kinetic parameters of the two electron transfer processes in terph$(S_2)_2$, digital simulations of the CV data were performed, applying a Butler–Volmer model over a scan-rate range of 0.1 V/s to 2 V/s.[74] A selection of representative experimental CV data (black traces) and corresponding simulated data (red dashed lines) are shown in Figure 3. Simulations of cyclic voltammograms with several other potential scan rates as well as with different potential sweep windows are shown in Figure S17 and Figure S18.

Good simulations were achieved by modeling four consecutive irreversible electron transfer events using the minimum model shown in Scheme S1 with the parameter values summarized in Table 1. To model the oxidative current, an

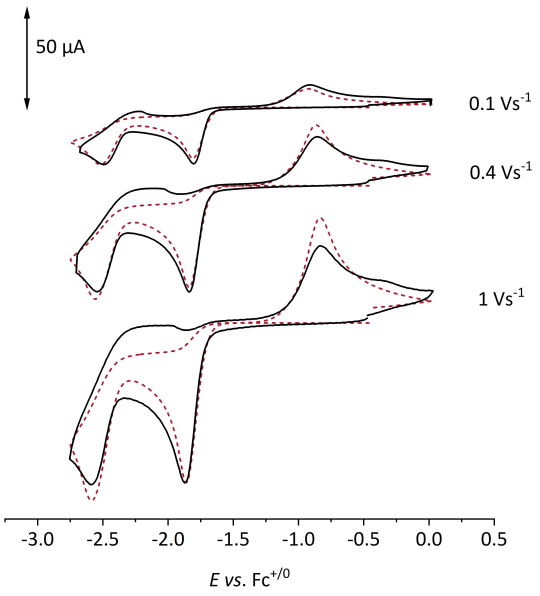

Figure 3. Cyclic voltammograms of 1.0 mM terph$(S_2)_2$ in dry, N_2-saturated THF at room temperature with 0.2 M (^{n}Bu$_4$N)(PF_6) as supporting electrolyte. Black lines: experimental data; red dashed lines: simulations with the parameters listed in Table 1.

Table 1. Thermodynamic and kinetic parameters obtained from the simulations of the CV data of terph$(S_2)_2$ describing the stepwise (n = 1–4) fourfold reduction.

n	E_n/V	α_n[a]	$k_{s,n}$[b]/cm s^{-1}
1	−1.55	0.65	$4\cdot10^{-5}$
2	−1.55	0.70	$7\cdot10^{-6}$
3	−1.85	0.55	$2\cdot10^{-8}$
4	−1.72	0.50	$1\cdot10^{-9}$

[a] α is the transfer coefficient, $0 < \alpha < 1$. [b] k_s is the electron transfer rate.

unproductive and slow pseudo-first-order chemical side reaction $k_c = 0.07\ s^{-1}$ of the fourfold reduced terph$(S_2)_2^{4-}$ had to be included, which likely reflects the partial protonation of this species due to traces of water in the electrolyte solution.[52,56]

Both reduction waves are steep (Figure 3) and the corresponding reoxidation feature is rather broad, pointing towards a transfer coefficient α of 0.5 or higher, at least for one of the two electron transfer processes of each observable wave. Indeed, reasonable simulations were achieved when the α values of the four individual single electron transfer events ($n =$ 1–4) were set to 0.65, 0.70, 0.55 and 0.50 (Table 1).[53] Transfer coefficients deviating from 0.5 imply asymmetric transition states and α values larger than 0.5 have been observed previously for related disulfide compounds.[51,56,57] The reductions of terph$(S_2)_2$ were all simulated as electrochemically irreversible processes to account for the large peak to peak separation, which is indicative for sizeable structural changes associated with the overall reduction. This is in line with the fact that in comparable disulfide compounds, the first reducing equivalent leads to substantial electron density in the σ*-antibonding orbital of the S–S bond, which causes bond elongation and consequently increased tilting of the aromatic units along the central C–C bond of a given biphenyl unit.[22,54–56] Uptake of the second electron was previously associated with S–S bond rupture and further rotation around the central C–C bond, in order to balance Coulombic repulsion between the two thiolate groups and steric interactions between two connected phenyl subunits.[22,54–56] Due to the chemical similarities between terph$(S_2)_2$ and the previously reported systems in Figure 1,[22,51–57] it seems reasonable to assume that similar structural changes occur upon two-electron reduction of terph$(S_2)_2$, leading to electrochemical irreversibility of the electron transfer reactions.[51–53,57]

According to the simulations, the first reduction occurs at a potential $E_1 = -1.55$ V and the second reduction requires the same potential $E_2 = -1.55$ V (Table 1). This is in agreement with literature reports on comparable disulfide-based systems, where the second reduction occurs at essentially the same (potential compression) or a less negative potential than the first reduction (potential inversion) due to the large structural changes.[51–57] The peak current of the first reduction wave of terph$(S_2)_2$ is similar to the peak current observed for related disulfide-biphenyl[22,55,56,59] and -bipyridine[52,54] systems, suggesting that the initial two-electron reduction induces S–S bond cleavage in one of the two disulfide moieties of terph$(S_2)_2$, leading to a dithiolate species. The third and fourth reductions were simulated with potentials of $E_3 = -1.85$ V and $E_4 = -1.72$ V, indicating potential inversion. These results support the hypothesis of two consecutive two-electron reductions of both disulfide units leading to S–S bond cleavage and the formation of a tetrathiolate species under electrochemical conditions.

UV-Vis absorption spectroscopy and photochemical reduction

The UV-Vis spectrum of terph$(S_2)_2$ features a prominent peak at 310 nm as well as absorption bands ranging into the visible part of the spectrum (Figure 4). To identify the UV-Vis spectral signatures of the twofold (terph$(S_2)_2^{2-}$) and fourfold (terph$(S_2)_2^{4-}$) reduced (bis)disulfide species, we employed electrochemical reduction in combination with UV-Vis absorption spectroscopy. Controlled potential coulometry of a 50 μM solution of terph$(S_2)_2$ in THF under inert atmosphere at a potential between the first and second reduction wave for 80 minutes resulted in the formation of terph$(S_2)_2^{2-}$.This species shows a new, broad absorption band with λ_{max} at 448 nm (green trace in Figure 4), which vanishes again upon further two-electron reduction to terph$(S_2)_2^{4-}$ (black trace in Figure 4).

Next, we set out to investigate the ability of terph$(S_2)_2$ to undergo photoinduced accumulation of multiple electrons. Given the very negative third and fourth reduction potentials of terph$(S_2)_2$ (see above), we chose tetrakis(dimethylamino)ethylene (TDAE) as a photoreductant, due to its exceptionally high excited-state oxidation potential of ca. −3.8 V vs. $Fc^{+/0}$.[75] TDAE has been previously employed as a stoichiometric photoreductant in energetically highly unfavorable radical-type hydrodehalogenation reactions.[76] In principle, TDAE is not an efficient light-harvesting chromophore, and the rationale for using this particular photoreductant is its unusually negative excited-state oxidation potential. In a first experiment, a solution of 3.3 mM terph$(S_2)_2$ and 5 equivalents of TDAE in C_6D_6 was irradiated with a 440 nm LED with a power output of 40 W. This led to the reduction of terph$(S_2)_2$ and extrusion of sulfur (likely in the form of sulfide),[53] yielding the thiophene species terph(S)(S_2) after an irradiation time of 24 h (Figure 5b and Figure S19). The photochemical formation of terph(S)(S_2) was confirmed by high-resolution ESI mass spectrometry (see SI, page S23) in addition to ^{1}H NMR spectroscopy. Thiophene formation in aromatic disulfide-based electron acceptors is known to take place at elevated temperatures or under reductive conditions.[54,57] In our case, it is conceivable that terph(S)(S_2) forms in two steps, via excitation of the twofold reduced terph$(S_2)_2^{2-}$. This dithiolate species features the above-mentioned absorption band between 400 and 550 nm (green

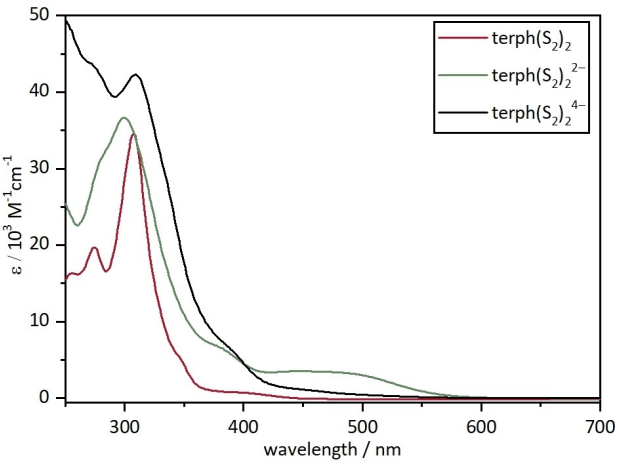

Figure 4. UV-Vis absorption spectra of terph$(S_2)_2$, terph$(S_2)_2^{2-}$ and terph$(S_2)_2^{4-}$ obtained through electrochemical reduction at room temperature in dry, Ar-saturated THF containing 0.2 M (nBu$_4$N)(PF_6).

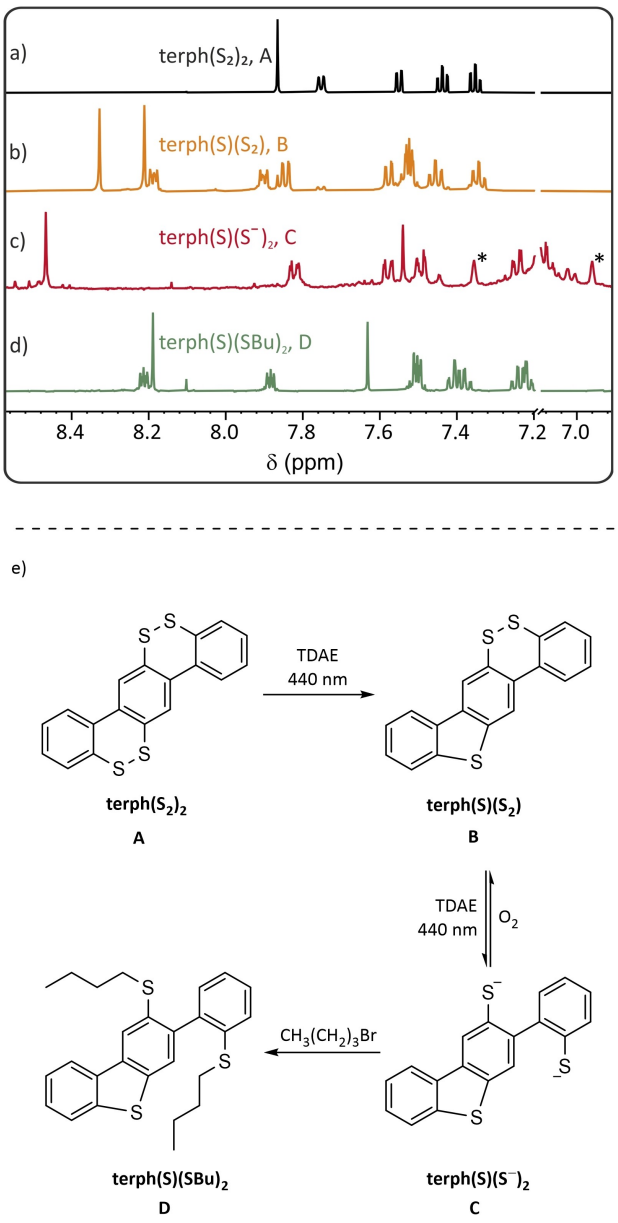

Figure 5. Top: Aromatic regions of the ^{1}H NMR spectra of the different species (A, B, C and D) obtained from photochemical reduction of terph$(S_2)_2$ (A) with the strong excited-state reductant TDAE in dry, Ar-saturated C_6D_6 under irradiation with a 440 nm LED at room temperature. The spectra shown in panels a, b and d were recorded in CD_2Cl_2 after work-up, whereas the spectrum shown in panel c was recorded in C_6D_6 without work-up. The region of the solvent residual peak of C_6D_6 (7.1–7.2 ppm) is omitted from the spectra for clarity. The asterisks in panel c mark the ^{13}C satellites of the solvent residual peak of C_6D_6. Bottom, e) Reactivity of terph$(S_2)_2$ based on the experimental data shown in panels a to d.

trace in Figure 4) and hence could absorb the 440 nm LED light directly. Consequently, it seems possible that following initial twofold reduction of terph$(S_2)_2$ to terph$(S_2)_2^{2-}$ via photoexcited TDAE, subsequent direct excitation of dithiolate terph$(S_2)_2^{2-}$ triggers sulfur extrusion to result in the formation of the thiophene terph(S)(S_2). Because terph$(S_2)_2$ also absorbs at 440 nm (Figure 4), it is furthermore possible that the initial reduction step occurs via direct excitation and subsequent reductive quenching of terph$(S_2)_2$ by TDAE.

When we increased the TDAE concentration from 5 to 15 equivalents, but kept all other reaction conditions constant, the formation of terph(S)(S_2) was markedly faster, reaching its peak concentration already after a reaction time of 9 h (68% NMR-yield, Figure 6). At even longer reaction times, the conversion of terph(S)(S_2) to yet another species started to become detectable (Figure 6), manifesting by a new set of signals in the aromatic region of the ^{1}H NMR spectrum of the reaction mixture (Figure S23). The appearance of these new signals parallels the disappearance of the terph(S)(S_2) resonances (Figure 6), suggesting that conversion of terph(S)(S_2) to the new species occurs in a consecutive A→B→C overall reaction process, in which A is terph$(S_2)_2$ and B is terph(S)(S_2) (Figure 5).

After a reaction time of 45 h, no terph$(S_2)_2$ or terph(S)(S_2) was present anymore and the new species C was dominant in the respective ^{1}H NMR spectrum (Figure 5c and Figure S23). However, when the reaction mixture containing species C was exposed to air, a fast reaction back to terph(S)(S_2) (species B) was observed, as confirmed by ^{1}H NMR spectroscopy (Figure S22). Thus it seems plausible that species C is the thiophene-dithiolate terph(S)$(S^-)_2$, because dithiolates are usually easily oxidized under air.[54] The oxygen-sensitive nature of the supposed terph(S)$(S^-)_2$ photoproduct did not allow further direct analysis and consequently, in Figure 5c, the ^{1}H NMR spectrum of the reaction mixture containing terph(S)$(S^-)_2$ is shown, whereas Figure 5b and d contain the spectra of the air-stable reaction products after work-up. To circumvent the oxygen-sensitivity issue, we aimed to intercept the presumed species C, in order to obtain a stable compound that can be properly characterized. Since thiolates are usually strong nucleophiles,[77] we anticipated that 1-bromobutane would readily react with terph(S)$(S^-)_2$ to form a characterizable doubly alkylated product. Adding 7 equivalents of degassed 1-bromobutane to a solution of terph(S)$(S^-)_2$ (prepared photo-

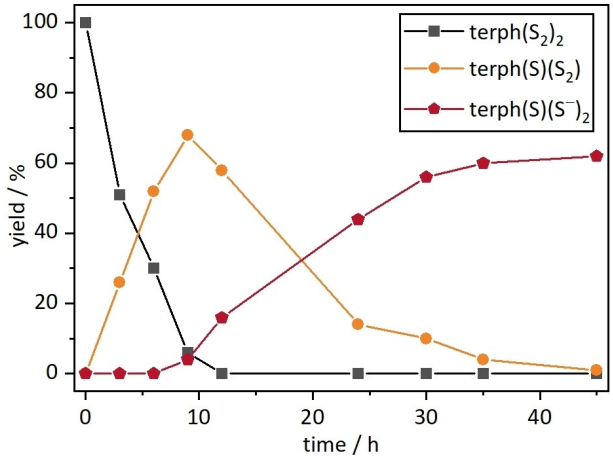

Figure 6. Yields of the different terphenyl species in the reduction of 3.3 mM terph$(S_2)_2$ with 15 equivalents of TDAE, performed in dry, deaerated C_6D_6 upon irradiation with a 440 nm LED at room temperature. Yields are reported with respect to the internal standard 1,3,5-trimethoxybenzene.

chemically according to procedure 3 in the SI) and heating the resulting solution to 40 °C for 28 h lead to formation of bench-stable terph(S)$(SBu)_2$ (Figure 5d) with 62% NMR yield determined relative to the internal standard 1,3,5-trimethoxybenzene. ^{1}H NMR and HRMS analysis (see SI, page S24) confirm the formation of terph(S)$(SBu)_2$, and we conclude that species C is indeed the terph(S)$(S^-)_2$ compound, as suspected above. It should be noted that the NMR-yield of terph(S)$(S^-)_2$ is only ca. 60%, whereas the starting material terph$(S_2)_2$ is completely consumed. We attribute this to possible deleterious reaction pathways, which could be due to the very reactive nature of photoexcited TDAE.

The results presented in this section illustrate that terph$(S_2)_2$ can not only be reduced electrochemically by up to four electrons but is furthermore able to undergo photoinduced multi-electron accumulation. The initial conversion of terph$(S_2)_2$ to terph(S)(S_2) likely occurs via formation of terph$(S_2)_2^{2-}$ with photoexcited TDAE, and direct light absorption by this dithiolate could then lead to the thiophene terph(S)(S_2) (species B), though the involved sequence of elementary steps cannot be fully elucidated. The subsequent two-electron reduction of terph(S)(S_2) to terph(S)$(S^-)_2$ presumably occurs by photoexcited TDAE. Importantly, terph$(S_2)_2$ did not participate in any reaction in the absence of light (Figure S27) or TDAE (Figure S28). Analogously to other aliphatic amines,[80] TDAE can be expected to act either as a one-electron or two-electron donor.

Conclusions

Photoinduced charge accumulation remains of considerable interest to mimic natural systems relevant for artificial photosynthesis and the production of solar fuels.[11–38,51–58,78,79] In order to expand the electron accumulation capacity of currently known molecular acceptors for the temporary storage of multiple redox equivalents, we report on the synthesis and characterization of the bis(disulfide) electron acceptor terph$(S_2)_2$, which can accumulate up to four electrons. Going beyond the previously achieved accumulation of two redox equivalents in molecular systems represents an important advance in the direction of mastering light-to-chemical energy conversion, complementing an early study of four-electron accumulation in a molecular compound.[18] Compared to that previously reported system, terph$(S_2)_2$ benefits from potential inversion and potential compression enabled by structural reorganizations in the course of its redox chemistry, which facilitate the uptake of four electrons by over-compensating Coulombic repulsion between the accumulated negative charges. Based on our study, the concepts of potential inversion and potential compression seem very promising for the accumulation and temporary storage of more than two redox equivalents under electro- and photochemical conditions.

Acknowledgements

This work was funded by the Swiss National Science Foundation through grant number 200020_207329. Funding from the Deutsche Forschungsgemeinschaft (DFG, SI 1577-5) is acknowledged. Open Access funding provided by Universität Basel.

Conflict of Interest

The authors declare no conflict of interest.

Data Availability Statement

The data that support the findings of this study are available in the supplementary material of this article.

Keywords: electron transfer · energy conversion · photochemistry · redox chemistry · UV/Vis spectroscopy

[1] M. R. Wasielewski, *Chem. Rev.* **1992**, *92*, 435–461.
[2] D. M. Guldi, *Chem. Soc. Rev.* **2002**, *31*, 22–36.
[3] C. Shih, A. K. Museth, M. Abrahamsson, A. M. Blanco-Rodriguez, A. J. Di Bilio, J. Sudhamsu, B. R. Crane, K. L. Ronayne, M. Towrie, A. Vlček, J. H. Richards, J. R. Winkler, H. B. Gray, *Science* **2008**, *320*, 1760–1762.
[4] M. B. Majewski, N. R. de Tacconi, F. M. MacDonnell, M. O. Wolf, *Chem. Eur. J.* **2013**, *19*, 8331–8341.
[5] J. Wiberg, L. Guo, K. Pettersson, D. Nilsson, T. Ljungdahl, J. Mårtensson, B. Albinsson, *J. Am. Chem. Soc.* **2007**, *129*, 155–163.
[6] J. H. Klein, D. Schmidt, U. E. Steiner, C. Lambert, *J. Am. Chem. Soc.* **2015**, *137*, 11011–11021.
[7] J. Sukegawa, C. Schubert, X. Zhu, H. Tsuji, D. M. Guldi, E. Nakamura, *Nat. Chem.* **2014**, *6*, 899–905.
[8] K. Hu, A. D. Blair, E. J. Piechota, P. A. Schauer, R. N. Sampaio, F. G. L. Parlane, G. J. Meyer, C. P. Berlinguette, *Nat. Chem.* **2016**, *8*, 853–859.
[9] M. M. Waskasi, G. Kodis, A. L. Moore, T. A. Moore, D. Gust, D. V. Matyushov, *J. Am. Chem. Soc.* **2016**, *138*, 9251–9257.
[10] D. Bao, S. Upadhyayula, J. M. Larsen, B. Xia, B. Georgieva, V. Nuñez, E. M. Espinoza, J. D. Hartman, M. Wurch, A. Chang, C.-K. Lin, J. Larkin, K. Vasquez, G. J. O. Beran, V. I. Vullev, *J. Am. Chem. Soc.* **2014**, *136*, 12966–12973.
[11] A. M. Appel, J. E. Bercaw, A. B. Bocarsly, H. Dobbek, D. L. DuBois, M. Dupuis, J. G. Ferry, E. Fujita, R. Hille, P. J. A. Kenis, C. A. Kerfeld, R. H. Morris, C. H. F. Peden, A. R. Portis, S. W. Ragsdale, T. B. Rauchfuss, J. N. H. Reek, L. C. Seefeldt, R. K. Thauer, G. L. Waldrop, *Chem. Rev.* **2013**, *113*, 6621–6658.
[12] E. Fujita, *Coord. Chem. Rev.* **1999**, *185–186*, 373–384.
[13] J. H. Alstrum-Acevedo, M. K. Brennaman, T. J. Meyer, *Inorg. Chem.* **2005**, *44*, 6802–6827.
[14] W. T. Eckenhoff, R. Eisenberg, *Dalton Trans.* **2012**, *41*, 13004–13021.
[15] L. Hammarström, *Acc. Chem. Res.* **2015**, *48*, 840–850.
[16] M. G. Pfeffer, C. Müller, E. T. E. Kastl, A. K. Mengele, B. Bagemihl, S. S. Fauth, J. Habermehl, L. Petermann, M. Wächtler, M. Schulz, D. Chartrand, F. Laverdière, P. Seeber, S. Kupfer, S. Gräfe, G. S. Hanan, J. G. Vos, B. Dietzek-Ivanšić, S. Rau, *Nat. Chem.* **2022**, *14*, 500–506.
[17] Y. Pellegrin, F. Odobel, *Coord. Chem. Rev.* **2011**, *255*, 2578–2593.
[18] R. Konduri, H. Ye, F. M. MacDonnell, S. Serroni, S. Campagna, K. Rajeshwar, *Angew. Chem. Int. Ed.* **2002**, *41*, 3185–3187; *Angew. Chem.* **2002**, *114*, 3317–3319.
[19] C. Chiorboli, S. Fracasso, F. Scandola, S. Campagna, S. Serroni, R. Konduri, F. M. MacDonnell, *Chem. Commun.* **2003**, 1658–1659.
[20] T. H. Bürgin, O. S. Wenger, *Energy Fuels* **2021**, *35*, 18848–18856.
[21] M. P. O'Neil, M. P. Niemczyk, W. A. Svec, D. Gosztola, G. L. Gaines, M. R. Wasielewski, *Science* **1992**, *257*, 63–65.
[22] J. Nomrowski, O. S. Wenger, *J. Am. Chem. Soc.* **2018**, *140*, 5343–5346.

[23] M. Orazietti, M. Kuss-Petermann, P. Hamm, O. S. Wenger, *Angew. Chem. Int. Ed.* **2016**, *55*, 9407–9410; *Angew. Chem.* **2016**, *128*, 9553–9556.
[24] H. Imahori, M. Hasegawa, S. Taniguchi, M. Aoki, T. Okada, Y. Sakata, *Chem. Lett.* **1998**, *27*, 721–722.
[25] J.-F. Lefebvre, J. Schindler, P. Traber, Y. Zhang, S. Kupfer, S. Gräfe, I. Baussanne, M. Demeunynck, J.-M. Mouesca, S. Gambarelli, V. Artero, B. Dietzek, M. Chavarot-Kerlidou, *Chem. Sci.* **2018**, *9*, 4152–4159.
[26] B. Matt, J. Fize, J. Moussa, H. Amouri, A. Pereira, V. Artero, G. Izzet, A. Proust, *Energy Environ. Sci.* **2013**, *6*, 1504–1508.
[27] M. Schulz, N. Hagmeyer, F. Wehmeyer, G. Lowe, M. Rosenkranz, B. Seidler, A. Popov, C. Streb, J. G. Vos, B. Dietzek, *J. Am. Chem. Soc.* **2020**, *142*, 15722–15728.
[28] A. Pannwitz, O. S. Wenger, *Chem. Commun.* **2019**, *55*, 4004–4014.
[29] R. Konduri, N. R. De Tacconi, K. Rajeshwar, F. M. MacDonnell, *J. Am. Chem. Soc.* **2004**, *126*, 11621–11629.
[30] M. Kuss-Petermann, M. Orazietti, M. Neuburger, P. Hamm, O. S. Wenger, *J. Am. Chem. Soc.* **2017**, *139*, 5225–5232.
[31] S. Karlsson, J. Boixel, Y. Pellegrin, E. Blart, H.-C. Becker, F. Odobel, L. Hammarström, *J. Am. Chem. Soc.* **2010**, *132*, 17977–17979.
[32] S. Karlsson, J. Boixel, Y. Pellegrin, E. Blart, H.-C. Becker, F. Odobel, L. Hammarström, *Faraday Discuss.* **2012**, *155*, 233–252.
[33] H. Kim, B. Keller, R. Ho–Wu, N. Abeyasinghe, R. J. Vázquez, T. Goodson, P. M. Zimmerman, *J. Am. Chem. Soc.* **2018**, *140*, 7760–7763.
[34] G. F. Manbeck, K. J. Brewer, *Coord. Chem. Rev.* **2013**, *257*, 1660–1675.
[35] G. Knör, A. Vogler, S. Roffia, F. Paolucci, V. Balzani, *Chem. Commun.* **1996**, 1643–1644.
[36] P. Gotico, T. Tran, A. Baron, B. Vauzeilles, C. Lefumeux, M. Ha-Thi, T. Pino, Z. Halime, A. Quaranta, W. Leibl, A. Aukauloo, *ChemPhotoChem* **2021**, *5*, 654–664.
[37] T.-T. Tran, M.-H. Ha-Thi, T. Pino, A. Quaranta, C. Lefumeux, W. Leibl, A. Aukauloo, *J. Phys. Chem. Lett.* **2018**, *9*, 1086–1091.
[38] S. Mendes Marinho, M.-H. Ha-Thi, V.-T. Pham, A. Quaranta, T. Pino, C. Lefumeux, T. Chamaillé, W. Leibl, A. Aukauloo, *Angew. Chem. Int. Ed.* **2017**, *56*, 15936–15940; *Angew. Chem.* **2017**, *129*, 16152–16156.
[39] D. H. Evans, *Chem. Rev.* **2008**, *108*, 2113–2144.
[40] Š. Lachmanová, G. Dupeyre, J. Tarábek, P. Ochsenbein, C. Perruchot, I. Ciofini, M. Hromadová, L. Pospíšil, P. P. Lainé, *J. Am. Chem. Soc.* **2015**, *137*, 11349–11364.
[41] D. H. Evans, K. Hu, *J. Chem. Soc., Faraday Trans.* **1996**, *92*, 3983.
[42] A. Gosset, L. Wilbraham, Š. N. Lachmanová, R. Sokolová, G. Dupeyre, F. Tuyèras, P. Ochsenbein, C. Perruchot, H.-P. J. de Rouville, H. Randriamahazaka, L. Pospíšil, I. Ciofini, M. Hromadová, P. P. Lainé, *J. Am. Chem. Soc.* **2020**, *142*, 5162–5176.
[43] N. A. Macías-Ruvalcaba, D. H. Evans, *J. Phys. Chem. B* **2006**, *110*, 5155–5160.
[44] T. Kitagawa, A. Ichimura, *Bull. Chem. Soc. Jpn.* **1973**, *46*, 3792–3795.
[45] C. Kraiya, D. H. Evans, *J. Electroanal. Chem.* **2004**, *565*, 29–35.
[46] M. W. Lehmann, P. Singh, D. H. Evans, *J. Electroanal. Chem.* **2003**, *549*, 137–143.
[47] J. L. Yuly, P. Zhang, X. Ru, K. Terai, N. Singh, D. N. Beratan, *Chem* **2021**, *7*, 1870–1886.
[48] F. Baymann, B. Schoepp-Cothenet, S. Duval, M. Guiral, M. Brugna, C. Baffert, M. J. Russell, W. Nitschke, *Front. Microbiol.* **2018**, *9*, 1357.
[49] D. H. Evans, P. M. Juusola, P. O. Minkkinen, C. E. Olsen, I. Søtofte, G. W. Francis, J. Szúnyog, B. Långström, *Acta Chem. Scand.* **1998**, *52*, 194–197.
[50] S. Muratsugu, K. Sodeyama, F. Kitamura, S. Tsukada, M. Tada, S. Tsuneyuki, H. Nishihara, *Chem. Sci.* **2011**, *2*, 1960.
[51] G. B. Hall, R. Kottani, G. A. N. Felton, T. Yamamoto, D. H. Evans, R. S. Glass, D. L. Lichtenberger, *J. Am. Chem. Soc.* **2014**, *136*, 4012–4018.
[52] M. Cattaneo, C. E. Schiewer, A. Schober, S. Dechert, I. Siewert, F. Meyer, *Chem. Eur. J.* **2018**, *24*, 4864–4870.
[53] S.-A. Hua, L. A. Paul, M. Oelschlegel, S. Dechert, F. Meyer, I. Siewert, *J. Am. Chem. Soc.* **2021**, *143*, 6238–6247.
[54] A. C. Benniston, J. Hagon, X. He, S. Yang, R. W. Harrington, *Org. Lett.* **2012**, *14*, 506–509.
[55] I. Llarena, A. C. Benniston, G. Izzet, D. B. Rewinska, R. W. Harrington, W. Clegg, *Tetrahedron Lett.* **2006**, *47*, 9135–9138.
[56] A. C. Benniston, B. D. Allen, A. Harriman, I. Llarena, J. P. Rostron, B. Stewart, *New J. Chem.* **2009**, *33*, 417–427.
[57] S.-A. Hua, M. Cattaneo, M. Oelschlegel, M. Heindl, L. Schmid, S. Dechert, O. S. Wenger, I. Siewert, L. González, F. Meyer, *Inorg. Chem.* **2020**, *59*, 4972–4984.
[58] J. Nomrowski, X. Guo, O. S. Wenger, *Chem. Eur. J.* **2018**, *24*, 14084–14087.
[59] Q. Zhu-Ohlbach, R. Gleiter, F. Rominger, H.-L. Schmidt, T. Reda, *Eur. J. Org. Chem.* **1998**, *1998*, 2409–2416.
[60] C. N. Valdez, A. M. Schimpf, D. R. Gamelin, J. M. Mayer, *J. Am. Chem. Soc.* **2016**, *138*, 1377–1385.
[61] C. N. Valdez, M. Braten, A. Soria, D. R. Gamelin, J. M. Mayer, *J. Am. Chem. Soc.* **2013**, *135*, 8492–8495.
[62] X.-B. Li, Y.-J. Gao, Y. Wang, F. Zhan, X.-Y. Zhang, Q.-Y. Kong, N.-J. Zhao, Q. Guo, H.-L. Wu, Z.-J. Li, Y. Tao, J.-P. Zhang, B. Chen, C.-H. Tung, L.-Z. Wu, *J. Am. Chem. Soc.* **2017**, *139*, 4789–4796.
[63] J.-J. Chen, M. D. Symes, L. Cronin, *Nat. Chem.* **2018**, *10*, 1042–1047.
[64] K. Yamamoto, A. Call, K. Sakai, *Chem. Eur. J.* **2018**, *24*, 16620–16629.
[65] K. Kitamoto, M. Ogawa, G. Ajayakumar, S. Masaoka, H.-B. Kraatz, K. Sakai, *Inorg. Chem. Front.* **2016**, *3*, 671–680.
[66] P. Barathi, A. S. Kumar, *Langmuir* **2013**, *29*, 10617–10623.
[67] J. E. Almlof, M. W. Feyereisen, T. H. Jozefiak, L. L. Miller, *J. Am. Chem. Soc.* **1990**, *112*, 1206–1214.
[68] J. Shukla, M. R. Ajayakumar, Y. Kumar, P. Mukhopadhyay, *Chem. Commun.* **2018**, *54*, 900–903.
[69] H. Lissau, C. L. Andersen, F. E. Storm, M. Santella, O. Hammerich, T. Hansen, K. V. Mikkelsen, M. B. Nielsen, *Chem. Commun.* **2018**, *54*, 2763–2766.
[70] C. Sonnenschein, C. P. Ender, F. Wang, D. Schollmeyer, X. Feng, A. Narita, K. Müllen, *Chem. Eur. J.* **2020**, *26*, 8007–8011.
[71] K.-S. Lee, J.-S. Lee, *Chem. Mater.* **2006**, *18*, 4519–4525.
[72] B. Zeysing, C. Gosch, A. Terfort, *Org. Lett.* **2000**, *2*, 1843–1845.
[73] A. J. Bard, L. R. Faulkner, *Electrochemical Methods: Fundamentals and Applications*, Wiley, New York, **2001**.
[74] M. C. Henstridge, E. Laborda, N. V. Rees, R. G. Compton, *Electrochim. Acta* **2012**, *84*, 12–20.
[75] Z. Zhao, F. Niu, P. Li, H. Wang, Z. Zhang, G. J. Meyer, K. Hu, *J. Am. Chem. Soc.* **2022**, *144*, 7043–7047.
[76] F. Glaser, C. B. Larsen, C. Kerzig, O. S. Wenger, *Photochem. Photobiol. Sci.* **2020**, *19*, 1035–1041.
[77] C. E. Hoyle, A. B. Lowe, C. N. Bowman, *Chem. Soc. Rev.* **2010**, *39*, 1355–1387.
[78] T. Sawaki, T. Ishizuka, N. Namura, D. Hong, M. Miyanishi, Y. Shiota, H. Kotani, K. Yoshizawa, J. Jung, S. Fukuzumi, T. Kojima, *Dalton Trans.* **2020**, *49*, 17230–17242.
[79] Z. Han, T. P. Vaid, A. L. Rheingold, *J. Org. Chem.* **2008**, *73*, 445–450.
[80] P. J. DeLaive, T. K. Foreman, C. Giannotti, D. G. Whitten, *J. Am. Chem. Soc.* **1980**, *102*, 5627–5631.

Manuscript received: August 1, 2022
Version of record online: November 9, 2022